JOURNAL OF VIROLOGY, June 2006, p. 6061–6071 Vol. 80, No. 12
0022-538X/06/$08.00+0 doi:10.1128/JVI.02167-05

Rotavirus NSP4 Induces a Novel Vesicular Compartment Regulated by Calcium and Associated with Viroplasms

Z. Berkova,[1,2] S. E. Crawford,[1] G. Trugnan,[3] T. Yoshimori,[4] A. P. Morris,[2]* and M. K. Estes[1]*

Baylor College of Medicine, Department of Molecular Virology and Microbiology, One Baylor Plaza, Houston, Texas 77030[1]; University of Texas, Health Science Center, Department of Integrative Biology and Pharmacology, 6431 Fannin, Houston, Texas 77030[2]; INSERM UMR538, UPMC, CHU St. Antoine, 27 rue Chaligny, 75014 Paris, France[3]; and National Institute of Genetics, Department of Cell Genetics, 1111, Yata, Mishima, Shizuoka 411-8540, Japan[4]

Received 14 October 2005/Accepted 22 March 2006

Rotavirus is a major cause of infantile viral gastroenteritis. Rotavirus nonstructural protein 4 (NSP4) has pleiotropic properties and functions in viral morphogenesis as well as pathogenesis. Recent reports show that the inhibition of NSP4 expression by small interfering RNAs leads to alteration of the production and distribution of other viral proteins and mRNA synthesis, suggesting that NSP4 also affects virus replication by unknown mechanisms. This report describes studies aimed at correlating the localization of intracellular NSP4 in cells with its functions. To be able to follow the localization of NSP4, we fused the C terminus of full-length NSP4 with the enhanced green fluorescent protein (EGFP) and expressed this fusion protein inducibly in a HEK 293-based cell line to avoid possible cytotoxicity. NSP4-EGFP was initially localized in the endoplasmic reticulum (ER) as documented by Endo H-sensitive glycosylation and colocalization with ER marker proteins. Only a small fraction of NSP4-EGFP colocalized with the ER-Golgi intermediate compartment (ERGIC) marker ERGIC-53. NSP4-EGFP did not enter the Golgi apparatus, in agreement with the Endo H sensitivity and a previous report that secretion of an NSP4 cleavage product generated in rotavirus-infected cells is not inhibited by brefeldin A. A significant population of expressed NSP4-EGFP was distributed in novel vesicular structures throughout the cytoplasm, not colocalizing with ER, ERGIC, Golgi, endosomal, or lysosomal markers, thus diverging from known biosynthetic pathways. The appearance of vesicular NSP4-EGFP was dependent on intracellular calcium levels, and vesicular NSP4-EGFP colocalized with the autophagosomal marker LC3. In rotavirus-infected cells, NSP4 colocalized with LC3 in cap-like structures associated with viroplasms, the site of nascent viral RNA replication, suggesting a possible new mechanism for the involvement of NSP4 in virus replication.

Rotavirus causes an age-dependent and potentially life-threatening dehydrating viral gastroenteritis in small animals and young children worldwide. The mechanism of rotavirus-induced diarrhea is not fully understood, but it is caused in part by the first described viral enterotoxin—rotavirus nonstructural protein 4 (NSP4) (3, 11). NSP4 has pleiotropic properties in cells related to its involvement in both rotavirus pathogenesis and morphogenesis (reviewed in references 4 and 11). Peritoneal injection or luminal administration of NSP4 into 6- to 10-day-old mice causes an age- and dose-dependent diarrhea within hours after inoculation. This diarrhea is due to extracellular NSP4 stimulating a transient, receptor-mediated phospholipase C activation, leading to elevated intracellular calcium levels and subsequent chloride secretion (3, 8, 22). Further studies have shown that a 66-amino-acid (aa) NSP4 cleavage product, which retains enterotoxigenic activity, is secreted into the media of rotavirus-infected cells early postinfection by a brefeldin A resistant mechanism, suggesting the existence of a nonclassical pathway that bypasses the Golgi apparatus for extracellular $NSP4_{112–175}$ release (32). During virus morphogenesis, intracellular NSP4 (iNSP4) serves as an intracellular receptor for the budding of nascent, immature double-layered particles into the lumen of endoplasmic reticulum (ER), where virus maturation occurs (1, 20). Inhibition of iNSP4 expression using small interfering RNAs alters the cellular distribution of other viral proteins, including the formation of viroplasms, where virus replication occurs, and also modulates viral mRNA synthesis, suggesting an additional role for NSP4 in virus replication (18, 26). In this study, we sought to elucidate the intracellular localization of iNSP4 and correlate this localization with iNSP4 functions. To avoid cytotoxicity of overexpressed NSP4 in transient transfections (28) as well as the effects of transfecting reagents on cell membranes, we developed and used a HEK 293-based cell line expressing NSP4-enhanced green fluorescent protein (EGFP) under a doxycycline-inducible promoter (5).

Our results show that intracellular NSP4-EGFP localizes in novel vesicular structures, which contain an autophagosomal marker. These vesicles associate with viroplasms in virus-infected cells, and their formation is regulated by levels of intracellular calcium. A new model for the role of different pools of iNSP4 in rotavirus replication and assembly is proposed.

* Corresponding author. Mailing address for M. K. Estes: Baylor College of Medicine, Department of Molecular Virology and Microbiology, One Baylor Plaza, Houston, TX 77030-3404. Phone: (713) 798-3585. Fax: (713) 798-3586. E-mail: mestes@bcm.tmc.edu. Mailing address for A. P. Morris: UT-HSC Medical School, Department of Integrative Biology and Pharmacology, 6431 Fannin, Houston, TX 77030. Phone: (713) 500-6681. Fax: (713) 500-6699. E-mail: andrew.p.morris@uth.tmc.edu.

MATERIALS AND METHODS

Cloning of NSP4-EGFP fusion protein. Gene 10 of rotavirus strain SA11 (32) encoding NSP4 was cloned from virus using a TOPO TA cloning kit (Invitrogen

Corp., Carlsbad, CA). The NSP4 gene was then PCR-amplified using a 5′ end primer targeting nucleotides 1 to 24 of the gene (bold) and introducing an EcoRI restriction site (italics) at the 5′ end (5′-CG*GAATTC*TAGA**GGCTTTTAAAAG TTCTGTTCCGAG**-3′), a 3′ end primer annealing to nucleotides 552 to 566 (bold) to introduce an AvaI restriction site, and a linker consisting of three glycine residues (italics) at the 3′end of the gene (5′-A*CCCCGGGCCTCC***CAT TGCTGCAGTCAC**-3′). The PCR product was inserted into EcoRI and AgeI restriction sites of the pEGFP-N1 vector (Clontech Laboratories, Inc., Palo Alto, CA). The NSP4-EGFP fusion gene was recloned into EcoRI and XbaI sites of the pTRE vector (Clontech Laboratories, Inc., Palo Alto, CA), and the NSP4-EGFP sequence was confirmed by sequencing (SeqWright, Inc., Houston, TX).

Generation of HEK 293 Tet on inducible cell line expressing NSP4-EGFP. The pTRE NSP4-EGFP vector was transfected into HEK 293 "Tet-on" cells (Clontech Laboratories, Inc., Palo Alto, CA) together with the selection marker vector pTK-Hyg (Clontech Laboratories, Inc., Palo Alto, CA) in a 20:1 ratio using Lipofectamine Plus (Gibco BRL, Life Technologies, Inc., Gaithersburg, MD) according to the manufacturer's recommendations. The transfected cells were kept under hygromycin B (37.5 μg/ml) and Geneticin selection (100 μg/ml) (both from Gibco BRL, Life Technologies, Inc., Gaithersburg, MD) until visible colonies of resistant cells appeared. NSP4-EGFP expression was induced by adding 5 μg/ml of doxycycline (Sigma-Aldrich Co., St. Louis, MO), and positive colonies were picked for expansion.

The generated HEK 293 "Tet-on" cells inducibly expressing NSP4-EGFP (HEK 293/NSP4-EGFP cells) were maintained according to recommendations from Clontech Laboratories, Inc. Cells were kept at 37°C and 5% CO_2 in minimal essential medium—alpha modification (Sigma-Aldrich Co, St. Louis, MO), with 10% Tet system approved fetal bovine serum (FBS) (Clontech Laboratories, Inc., Palo Alto, CA), 2 mM L-glutamine (Sigma-Aldrich Co, St. Louis, MO), 100 μg/ml of Geneticin, and 37.5 μg/ml of hygromycin B (both from Gibco BRL, Life Technologies, Inc., Gaithersburg, MD). Cells were split at a ratio of 1:3 two times per week.

Enrichment of NSP4-EGFP-expressing population by fluorescence-activated cell sorting. To enhance the number of NSP4-EGFP-expressing HEK 293 "Tet-on" cells in the cultures, 5×10^5 clonal cells were seeded into one T-25 flask and induced 24 h postseeding with 5 μg/ml of doxycycline. Cells were collected 24 h after induction and suspended in 0.5 ml of cold 2% Tet system approved FBS (Clontech Laboratories, Inc., Palo Alto, CA) in 0.01 M phosphate-buffered saline (PBS). Cells were sorted using a Beckman-Coulter ALTRA (Beckman-Coulter, Inc., Fullerton, CA) with fluorescein isiothiocyanate filter setting. Cells with EGFP fluorescence were collected and expanded. The resulting cloned cells expressed NSP4-EGFP in about 80% of cells, but the expression decreased with each passage despite the presence of selective drugs in the maintenance medium.

Immunoprecipitation and Western blotting. For metabolic labeling, cells were starved for 1 h by replacing the regular medium with methionine- and cysteine-free Dulbecco's modified Eagle medium (Invitrogen Corp., Carlsbad, CA). The medium was aspirated and replaced with the same medium supplemented with 45 μCi/well of ^{35}S Redivue Pro-mix (Amersham Biosciences, Piscataway, NJ). Two hours later, cells were collected, lysed in 200 μl of RIPA buffer (0.15 M NaCl, 1%-sodium deoxycholate, 1% Triton X-100, 0.1% sodium dodecyl sulfate [SDS], 0.01 M Tris-HCl, pH 7.2, 1% Trasylol), and processed for immunoprecipitation with a rabbit anti-NSP4 peptide aa 120 to 147 antibody (anti-NSP4 120–147) (prepared in our laboratory [32]) or with a rabbit anti-green fluorescent protein (GFP) antibody (Clontech Laboratories, Inc., Palo Alto, CA) as described previously (9).

Western blot analysis was performed using lysates from induced cells and rabbit anti-NSP4 120–147 antibody followed by alkaline phosphatase-conjugated secondary goat anti-rabbit immunoglobulin G antibody (Sigma-Aldrich Co., St. Louis, MO). The membrane was developed according to manufacturer's recommendations.

Immunofluorescence and confocal microscopy. The HEK 293/NSP4-EGFP cells were seeded onto four chambered microscope slides (Nalgene Nunc International, Naperville, IL) (2×10^4 cells/chamber) and induced with 10 μg/ml of doxycycline at the time of seeding where indicated. Two hours post-seeding/induction, doxycycline-containing medium was replaced with regular growth medium. Twenty-four hours post-seeding/induction, cells were fixed with 4% formaldehyde in 0.01 M PBS for 30 min at 4°C and permeabilized with 0.5% Triton X-100 for 30 min. After three washes with PBS, slides were incubated with primary antibodies to organelle markers: mouse monoclonal antibodies to the ER-Golgi intermediate compartment (ERGIC) lectin ERGIC-53 (H. P. Hauri, Basel, Switzerland), to protein disulfide isomerase (PDI) localized in the ER lumen (StressGen Bioreagents, Victoria, British Columbia, Canada), to β-COP, to the Golgi membrane protein giantin (both from G. Trugnan, Paris, France), to the endosomal marker Rab9 (Abcam, Inc., Cambridge, MA), to β-tubulin (NeoMarkers, Fremont, CA), rabbit polyclonal antibodies to the ER membrane protein calnexin (StressGen Bioreagents, Victoria, British Columbia, Canada), to lysosomal proteins β-galactosidase (A. W. C. Einerhand, Rotterdam, The Netherlands) and LAMP1 (Abcam, Inc., Cambridge, MA), and to autophagosomal protein LC3 (16) and anti-NSP4 120–147 antibody (32) overnight at 4°C. Cells were washed three times with PBS and incubated with secondary Alexa 594-conjugated goat anti-mouse antibody or Alexa 594-conjugated donkey anti-rabbit antibody (Molecular Probes, Eugene, OR) for 4 h at room temperature. For labeling of the plasma membrane, cells were fixed as above, but the permeabilization step was omitted. After three washes in PBS, cells were stained with Texas Red-conjugated wheat germ agglutinin (TxRed-WGA) (Molecular Probes, Eugene, OR) for one hour at room temperature. After three washes in PBS and autofluorescence quenching by treatment with 1 mg/ml of $NaBH_4$ (Sigma-Aldrich Co., St. Louis, MO), slides were mounted in Vectashield mounting medium (Alexis PLATFORM, San Diego, CA) and sealed with clear nail polish.

Fixed cells were imaged with a Zeiss LSM 510 META confocal microscope using a ×63 immersion oil objective (Carl Zeiss, Germany) in the multitrack scanning mode with excitation wavelengths set at 488 nm (Argon laser), 543 nm, and 633 nm (HeNe lasers); emission wavelengths were 505 to 530 nm, >560 nm, >585 nm, and >640 nm for EGFP, Alexa 568, Alexa 594, and Alexa 647 signal detection, respectively. Single optical slices were set to 0.8 μM and Z-stack slices to 0.38 μM. Collected images were processed using LSM Image VisArt (Carl Zeiss, Inc., Thornwood, NY), exported in a 12-bit TIFF RGB format, and converted into CMYK color space using Adobe Photoshop 7.0 (Adobe Systems Inc., San Jose, CA).

Live cell experiments. For live cell experiments, cells were seeded onto poly-D-lysine (Sigma-Aldrich Co., St. Louis, MO)-coated coverslips (6×10^4 cells in 200 μl of culture medium per coverslip) and induced as above. Twenty-four hours post-seeding/induction, coverslips were mounted onto measurement chambers and continuously washed with Na-HEPES buffer supplemented with 1 mM $CaCl_2$ at 37°C (4). Cells were incubated with TxRed-WGA or with lipophilic dye RH414 (Molecular Probes, Eugene, OR). After a 5-min incubation at 37°C, cells were perfused with Na-HEPES buffer supplemented with 1 mM $CaCl_2$ to wash away unbound label, and internalization of the dye was followed with the Zeiss LSM 510 META confocal microscope at 1-min time intervals.

For live cell experiments requiring manipulation of the calcium concentration, cells were seeded as above. After a 2-h adherence and induction period, the medium was replaced with culture medium containing 2 mM EGTA to chelate calcium (calcium-free medium), and cells were grown for 24 h. After mounting coverslips into the measurement chambers, cells were perfused with Na-HEPES buffer without calcium and zero time-point images acquired. A calcium switch was generated by supplementing the perfusion buffer with 2 mM $CaCl_2$, and images were collected at indicated time points. To measure changes in intracellular calcium concentration, cells were loaded with Fura-2 upon mounting in measurement chambers, and a 340/380 ratio of Fura-2 fluorescence above 560 nm was recorded as described previously (5).

Transient transfection. NSP4 from rotavirus strain SA11 was cloned into pDsRed-Monomer-N1 vector (BD Biosciences Clontech, Palo Alto, CA) using a strategy identical to that described for cloning NSP4 into the pEGFP vector (see above). The identical set of primers was used to amplify NSP4 for insertion into EcoRI and AgeI restriction sites of the pDsRed-Monomer-N1 vector (Clontech Laboratories, Inc., Palo Alto, CA).

Cells were seeded onto chambered microscope slides (Nalgene Nunc International, Naperville, IL) at 50% confluence (1×10^4 cells/chamber) and transfected with 1 μg of LC3-GFP plasmid (15) and 2 μl of Lipofectamine 2000 per chamber as recommended by the manufacturer (Gibco BRL, Life Technologies, Inc., Gaithersburg, MD). Forty-eight hours posttransfection, cells were transfected by using the same method with 1 μg of NSP4-DsRed plasmid. Twenty-four hours later, cells were fixed with 4% formaldehyde for 20 min at 4°C. After three washes with PBS, slides were mounted as described above.

Virus infection. Cells were grown in Dulbecco's modified Eagle medium (Gibco BRL, Life Technologies, Inc., Gaithersburg, MD) supplemented with 10% fetal bovine serum. Serum-free medium was put on the cells 1 to 18 h before infection. Rotavirus strain SA114F, diluted in serum-free medium, was adsorbed onto cells for 1 h at 37°C at a multiplicity of infection (MOI) of 10. Upon removal of the inoculum, the cells were kept in serum-free medium or medium containing 10% FBS and fixed at 7 and 10 h postinfection as described above. Rotavirus nonstructural protein 5 (NSP5) was detected by staining with a polyclonal antibody developed in guinea pig by our laboratory (29) and by Alexa 568-conjugated goat anti-guinea pig secondary antibody (Molecular Probes, Eugene, OR), NSP4 was stained with mouse anti-NSP4 peptide 114–135 antibody and with Alexa 488-conjugated goat anti-mouse secondary antibody (Molecular Probes, Eugene,

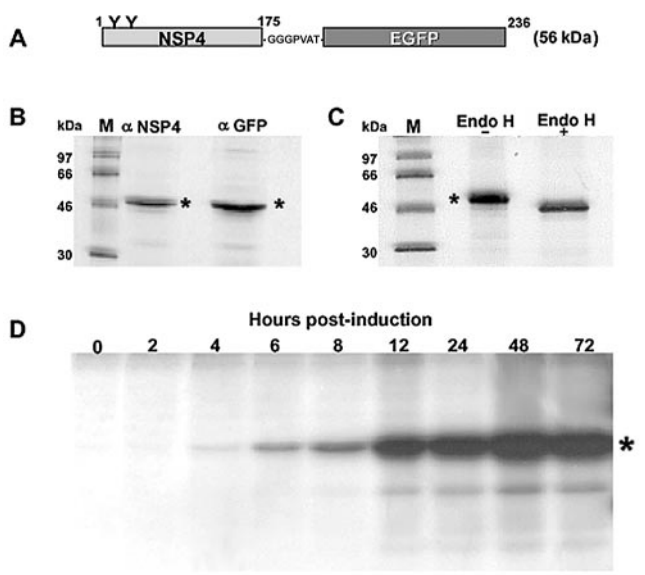

FIG. 1. Expression of NSP4-EGFP in inducible HEK 293/NSP4-EGFP cells. (A) Schematic diagram of NSP4-EGFP fusion protein; (B) autoradiograph of radiolabeled NSP4-EGFP immunoprecipitated from doxycycline-induced cells using anti-NSP4 120–147 and anti-GFP antibody; (C) autoradiograph of radiolabeled NSP4-EGFP immunoprecipitated with anti-NSP4 120–147 antibody without and with treatment with 500 units of Endo H for 1 h at 37°C; (D) autoradiograph of radiolabeled NSP4-EGFP precipitated with anti-NSP4 120–147 antibody at indicated times postinduction as described in Materials and Methods. *, fully glycosylated NSP4-EGFP.

OR), and LC-3 was stained using rabbit polyclonal anti-LC3 antibody and Alexa 647-conjugated donkey anti-rabbit antibody.

RESULTS

Glycosylated NSP4-EGFP protein is expressed in inducible cells. To study NSP4-EGFP protein expression in the inducible HEK 293 cell line, cells were induced with 5 μg/ml of doxycycline for 24 h, and induced protein was immunoprecipitated from cell lysates with rabbit anti-NSP4 120–147 and rabbit anti-GFP antibodies (Fig. 1). Both antibodies precipitated protein with a predicted size of 56 kDa (Fig. 1B). NSP4 contains a noncleavable ER-targeting signal peptide within its second hydrophobic domain (aa 28 to 47) and is cotranslationally N glycosylated at asparagine residues 8 and 18 (6, 9). To determine if NSP4-EGFP was posttranslationally glycosylated, immunoprecipitated NSP4-EGFP was subjected to Endo H digestion. NSP4-EGFP treated with Endo H migrated faster in an SDS-polyacrylamide gel, confirming the expected Endo H sensitivity (Fig. 1C). To study the kinetics of NSP4-EGFP expression, cells grown in medium supplemented with 5 μg/ml of doxycycline were metabolically labeled for 2 h at different time points after doxycycline addition, and the amount of de novo-synthesized protein was examined by electrophoresis on an SDS-polyacrylamide gel and by autoradiography. The NSP4-EGFP fusion protein was detected as early as 4 h postinduction, and the level of expression gradually increased up to 48 h postinduction (Fig. 1D). To avoid possible effects of doxycycline on the studied cells, a "short" induction time was evaluated in which cells were exposed to 10 μg/ml of doxycycline for 2 h and then incubated in doxycycline-free growth medium. Western blot analysis showed comparable amounts of NSP4-EGFP protein in cell lysates 24 h post-"short" induction and regular 24-h induction (data not shown). The "short" induction time was used in all subsequent experiments.

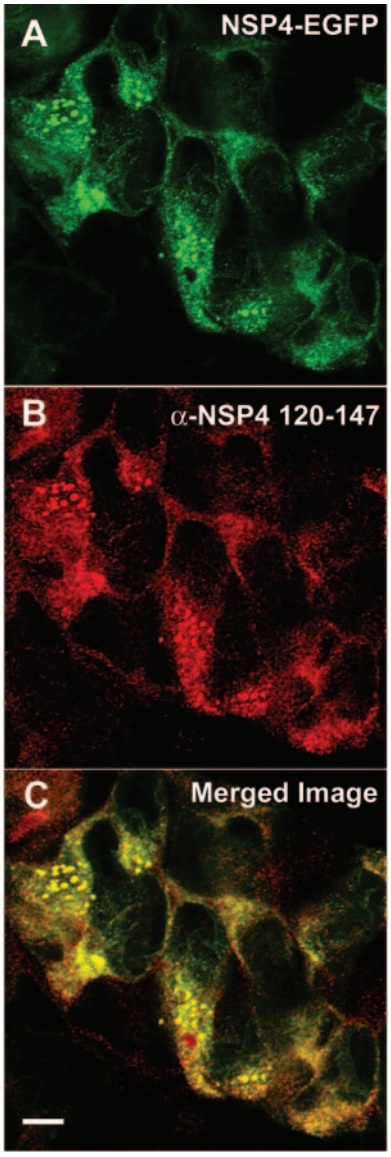

FIG. 2. All expressed NSP4-EGFP is recognized by rabbit anti-NSP4 120–147 antibody, and there is no intracellular NSP4 protein not fused with EGFP. HEK 293/NSP4-EGFP cells were induced for 24 h, fixed, and stained with rabbit anti-NSP4 120–147 antibody and anti-rabbit Alexa 594-conjugated secondary antibody as described in Materials and Methods. Stained cells were then observed by confocal microscopy. (A) NSP4-EGFP fluorescence; (B) immunofluorescence with anti-NSP4 120–147 antibody staining; (C) merged image of A and B. Bar = 15 μm.

Immunofluorescence of induced NSP4-EGFP-expressing cells using anti-NSP4 120–147 antibody showed that all EGFP fluorescence of the chimeric protein in these cells corresponded with the localization of the fusion protein (Fig. 2).

NSP4-EGFP is initially localized in the endoplasmic reticulum and does not enter the Golgi apparatus. To visualize the

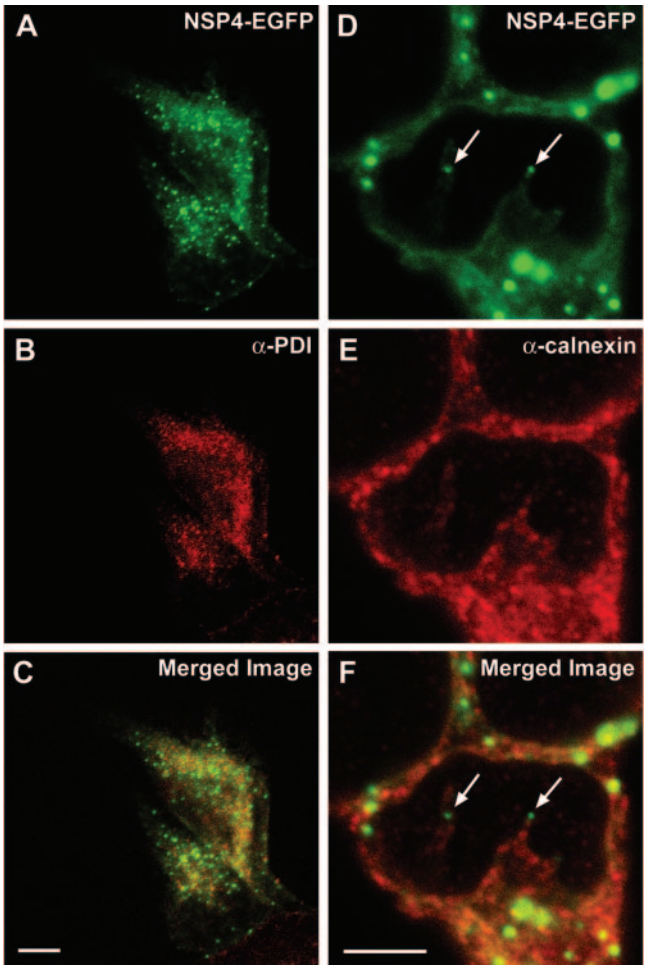

FIG. 3. Expressed NSP4-EGFP fusion protein is initially localized in the ER of HEK 293 cells. Cells were induced for 24 h, fixed, and stained with mouse monoclonal anti-PDI antibody (B, C) or rabbit anti-calnexin antibody (E, F) and corresponding Alexa 594-conjugated secondary antibody as described in Materials and Methods. Stained cells were then observed by confocal microscopy. (A, D) NSP4-EGFP fluorescence; (B) immunostaining of PDI; (C) merged image of A and B; (E) immunostaining of calnexin; (F) merged image of D and E. Arrows indicate NSP4-EGFP-positive, calnexin-negative vesicles in the vicinity of the ER. Bars = 10 μm.

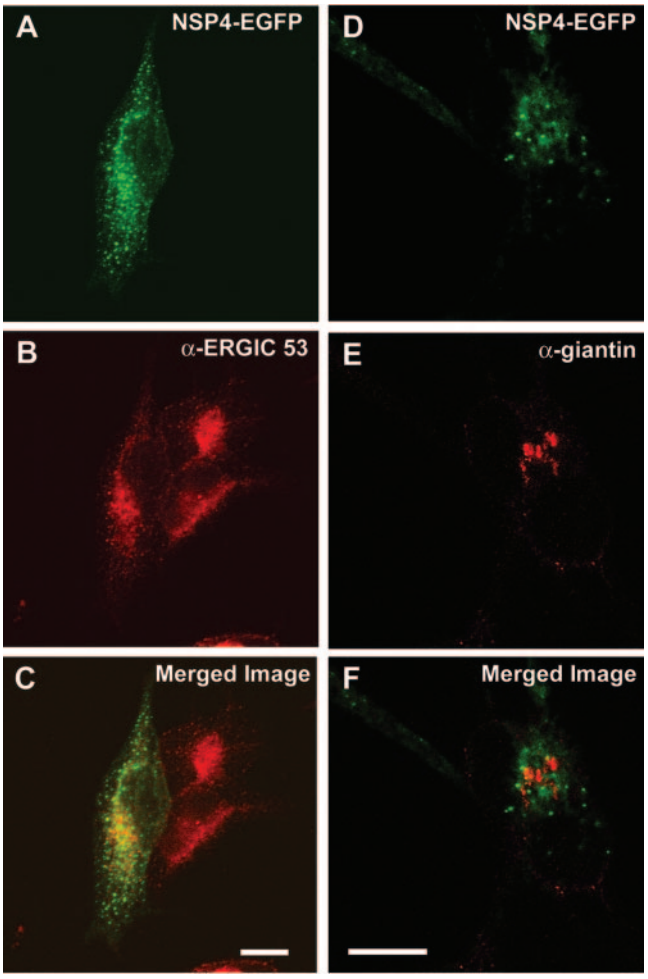

FIG. 4. Only a portion of vesicular NSP4-EGFP is localized within the ER-Golgi intermediate compartment, and no NSP4-EGFP enters the Golgi apparatus in HEK 293 cells. Cells were fixed 24 h postinduction and stained with mouse monoclonal antibody to ERGIC-53 or to giantin, followed by the Alexa 594-conjugated anti-mouse secondary antibody. Cells were then observed by confocal microscopy. (A, D) NSP4-EGFP fluorescence; (B) ERGIC-53 immunostaining; (C) merged image of A and B; (E) Golgi marker giantin staining; (F) merged image of D and E. Bars = 10 μm.

cellular localization of NSP4-EGFP fusion protein in the inducibly expressing HEK 293 cells relative to known biosynthetic pathways, we immunolabeled fixed, permeabilized cells with the ER markers PDI (Fig. 3A to C) and calnexin (Fig. 3D to F) 24 h postinduction. NSP4-EGFP fluorescence was detected as a diffuse staining pattern predominantly within the perinuclear region of the cells and as a punctate staining dispersed throughout the cytoplasm. Only a subset of NSP4, the diffusely distributed, perinuclearly localized, nonpunctate NSP4-EGFP, colocalized with both ER markers (Fig. 3). NSP4-EGFP localized in vesicular structures did not colocalize with calnexin. The yellow fluorescence signals in Fig. 3F do not represent colocalization but are caused by an overlap of signals from different depths of optical fields as illustrated by the different staining patterns in panels D and E. Panels D and F of Fig. 3 show NSP4-EGFP-positive but calnexin-negative puncta, marked by arrows, in the vicinity of the calnexin-positive ER membrane. The observed cytoplasmic punctate structures (size range, between 0.8 and 1.5 μm) thus lack ER markers. In addition, larger vesicular structures (3 to 4 μm in diameter) were observed at lower frequency.

A small pool of NSP4-EGFP colocalizes with the ER-Golgi intermediate compartment marker, but no NSP4-EGFP is localized in the Golgi apparatus. Xu et al. (31) reported that NSP4 transiently expressed in Cos-7 cells colocalizes with the ERGIC marker ERGIC-53 and a vesicular coat protein β-COP in anterograde vesicles aligned along microtubules. Using the same markers in the present study, we found that only a subset (approximately 30%) of cellular NSP4-EGFP colocalized with ERGIC-53 (Fig. 4A to C), and there was no detectable colocalization of NSP4-EGFP with β-COP (data not shown). The NSP4-EGFP vesicles were not aligned along microtubules and did not retract into the microtubule organiz-

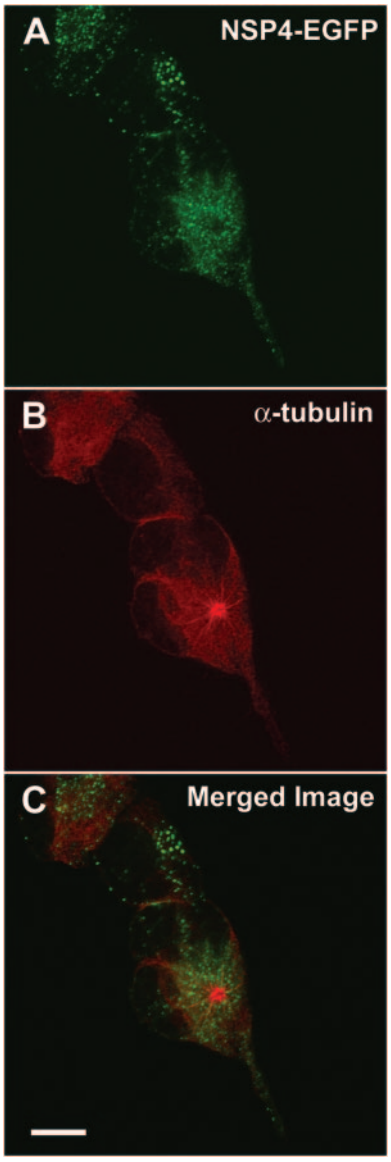

FIG. 5. NSP4-EGFP vesicles do not align along microtubules in HEK 293 cells. Cells were induced for 24 h, and 1 h prior to fixation and permeabilization the cells were kept at 4°C to induce coalescence of microtubules into MTOC. Cells were stained with mouse monoclonal antibody to β-tubulin, followed by the Alexa 594-conjugated anti-mouse secondary antibody. Cells were then observed by confocal microscopy. (A) NSP4-EGFP fluorescence; (B) β-tubulin immunostaining; (C) merged image of A and B. Bar = 10 μm.

ing center (MTOC) in cells incubated at 4°C for 1 h to block anterograde vesicle movement (Fig. 5). These results indicate that NSP4-EGFP-containing vesicles were not a part of the anterograde biosynthetic vesicular trafficking pathway and were thus distinct from vesicles described by Xu et al. (31). The ERGIC-53 staining was comparable in NSP4-EGFP-expressing and -nonexpressing cells (Fig. 4A to C), suggesting similar morphologies of the ERGIC compartment in the two types of cells. Double staining of NSP4-EGFP-expressing cells utilizing the ER marker calnexin and the ERGIC marker ERGIC-53 showed that a significant part of the NSP4-EGFP-containing vesicles distributed within the cytoplasm failed to colocalize with either marker (Fig. 6). In agreement with our glycosylation sensitivity experiments described above, NSP4-EGFP did not enter the Golgi apparatus (Fig. 4D to F). The fluorescence signals of NSP4 and the Golgi marker giantin were mutually exclusive (Fig. 4F), as expected from localization of NSP4-EGFP relative to MTOC (Fig. 5).

NSP4-EGFP does not enter endosomes and lysosomes. To characterize the ERGIC-53-negative, NSP4-EGFP-positive vesicles and to determine if they represent a post-ER vesicular compartment of any known biosynthetic pathway, we stained cells with the late endosomal marker Rab-9 (Fig. 7A to C) and lysosomal markers β-galactosidase (Fig. 7D to F) and LAMP1 (data not shown). No colocalization of NSP4-EGFP-containing vesicular structures with either of these markers was seen 24 and 48 h postinduction. When live cells were incubated with the lipophilic marker RH414 or TxRed-WGA, known to label the plasma membrane, endosomes, and lysosomes (14), no colocalization was observed at early time points (~5 min) postlabeling in plasma membrane and early endosomes. At thirty minutes postlabeling, when both markers enter late endosomes and lysosomes, no colocalization with NSP4-EGFP vesicles was observed despite efficient marker internalization (data not shown). Based on the complete overlap of EGFP and anti-NSP4 120–147 antibody staining in NSP4-EGFP-expressing cells (Fig. 2), lack of colocalization with the organelle markers was not due to loss of EGFP from the fusion protein but was due to a lack of physical colocalization, suggesting that NSP4-EGFP vesicles represent a novel vesicular compartment.

NSP4-EGFP can be detected close to, but not within, the plasma membrane. NSP4 EGFP was not detected in the plane of the plasma membrane either in live cells (above) or in fixed cells stained with TxRed-WGA or RH414. However, in both instances, NSP4-EGFP was seen to accumulate underneath the cytoplasmic leaflet of the plasma membrane (Fig. 8), although it did not colocalize with actin (Berkova et al., unpublished data). To examine if the observed cytoplasmic punctate staining represented vesicles and not protein aggregates, we incubated live cells with the detergent Triton X-100, known to disrupt membranes but to preserve EGFP fluorescence. After a 20-min incubation, the NSP4-EGFP puncta within the cytoplasm disappeared, leaving a diffuse cytoplasmic background staining, indicating the vesicular character of the punctate NSP4-EGFP staining.

NSP4-EGFP enters an alternative pathway labeled by the autophagosomal marker LC3. Xu et al. (30) reported that rotavirus infection, as well as the transient expression of NSP4 alone, upregulates the expression of the ER-localized chaperones BiP and endoplasmin. The authors attributed this phenomenon to ER stress. Thus, we tested the hypothesis that NSP4 vesicles are related to autophagy—ER-derived double-membrane vesicles known to be induced by stress (16). We stained induced cells with an antibody to the autophagosomal marker LC3 (16). Anti-LC3 antibody staining in NSP4-EGFP-negative cells was diffuse (Fig. 9B), without signs of vesiculation, while in NSP4-EGFP-expressing cells, LC3 always colocalized with NSP4-EGFP vesicles (Fig. 9C). To confirm that the observed colocalization was correct, we transfected HEK 293 cells with an LC3-GFP plasmid and 48 h later with an NSP4-DsRed plasmid. NSP4-DsRed colocalized with LC3-

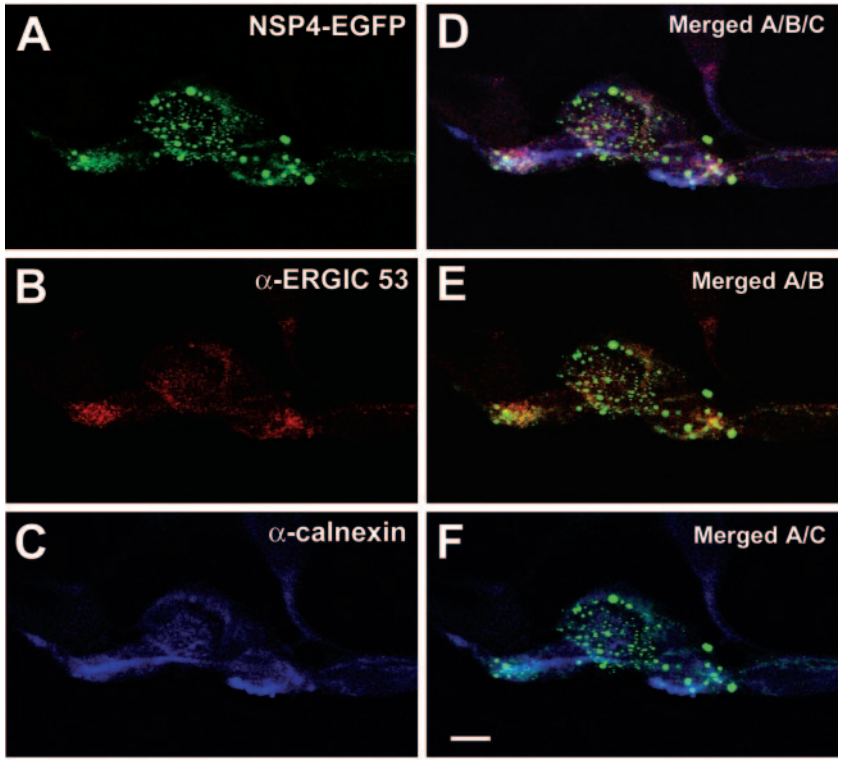

FIG. 6. A population of NSP4-EGFP fusion protein localizes in the ER or ERGIC compartment in HEK 293 cells. Cells were induced for 24 h, fixed, and stained with rabbit anti-calnexin and mouse monoclonal anti-ERGIC-53 antibodies, followed with Alexa 568-conjugated anti-mouse and Alexa 647-conjugated anti-rabbit antibodies. Cells were then observed by confocal microscopy. (A) NSP4-EGFP fluorescence; (B) immunostaining of ERGIC-53; (C) immunostaining of calnexin; (D) merged image of A, B, C; (E) merged image of A and B; (F) merged image of A and C. Bar = 10 μm.

GFP in large and small vesicles (Fig. 9D to F; the two images of the NSP4-positive cells shown were acquired separately).

NSP4 and autophagosomal marker-positive vesicles associate with viroplasms in rotavirus-infected cells. Our finding of NSP4 colocalization with the autophagosomal marker LC3 in NSP4-EGFP-expressing cells led us to question if this colocalization is relevant to rotavirus infection. Rotavirus SA114F-infected MA104 cells were fixed at 7 h postinfection and stained for NSP4, LC3, and a marker for rotavirus viroplasms (the sites of rotavirus RNA replication), NSP5. The autophagosomal marker LC3 clearly colocalized with NSP4 in rotavirus-infected cells. Moreover, LC3- and NSP4-positive structures were associated with NSP5-stained viroplasms (Fig. 10), forming cap-like structures on viroplasms, closely resembling NSP4 staining in rotavirus-infected cells described previously (13). These results were not the consequence of incubating rotavirus-infected cells in serum-free medium, since similar results were obtained in infected cells maintained in medium supplemented with 10% fetal bovine serum (data not shown). Localization of NSP4 in rotavirus-infected MA104 cells thus agreed with localization of NSP4-EGFP expressed in HEK 293 cells but was different from the previously reported localization of transiently expressed NSP4 in ERGIC-53 vesicles in Cos-7 cells (31). To address whether these differences were due to using different cell lines, we next studied localization of NSP4 in rotavirus-infected Cos-7 cells. Only limited colocalization of NSP4 with ERGIC (Fig. 11, panels A to C), but extensive colocalization of NSP4 with LC3 (Fig. 11, panels D to F), similar to the case with rotavirus-infected MA104 cells, was observed.

Formation of ER-derived NSP4-EGFP vesicles depends on elevated levels of intracellular calcium. Normal intracellular calcium is known to be required for the correct folding and movement of nascent glycoproteins through the constitutive biosynthetic pathway (7). We had shown previously that NSP4-EGFP-expressing HEK 293 cells possessed intracellular calcium levels more than twofold higher than those of nonexpressing cells (5). We therefore asked the question: does the intracellular calcium concentration affect the formation of NSP4-EGFP vesicles?

The vesicular distribution of NSP4-EGFP described above was observed in cells grown in normal (2 mM) calcium-containing medium. In the absence of extracellular calcium (culture medium plus 2 mM EGTA), NSP4-EGFP localization was restricted to a diffuse staining pattern (Fig. 12A). Normalization of extracellular calcium triggered by addition of 2 mM $CaCl_2$ into the perfusion buffer (Fig. 12B) resulted in formation of NSP4-EGFP vesicles within 5 min (Fig. 12A). Thus, NSP4-EGFP vesicle formation is induced by elevated intracellular calcium levels.

DISCUSSION

Rotavirus nonstructural protein 4 functions in both viral morphogenesis and pathogenesis (4, 11). Recent reports show that small interfering RNA inhibition of NSP4 expression in

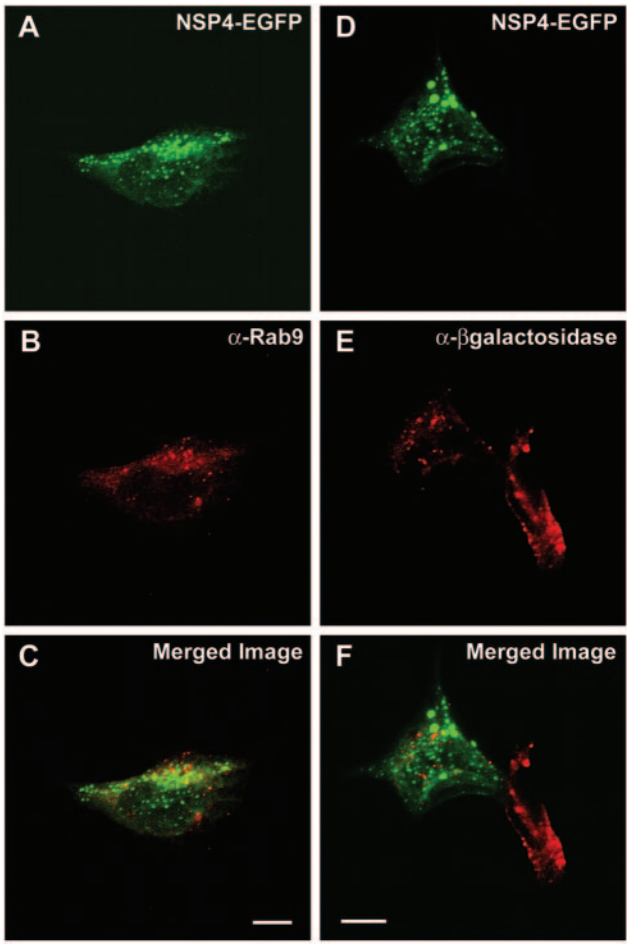

FIG. 7. NSP4-EGFP does not localize in endosomes or lysosomes of HEK 293 cells. Fixed and permeabilized cells, 24 h postinduction, were stained with mouse anti-Rab9 or rabbit anti-β-galactosidase antibody and the corresponding Alexa 594-conjugated secondary antibody. (A, D) NSP4-EGFP fluorescence; (B) lysosomal β-galactosidase staining; (C) merged image of A and B; (E) endosomal marker Rab9 staining; (F) merged image of D and E. Bars = 10 μm.

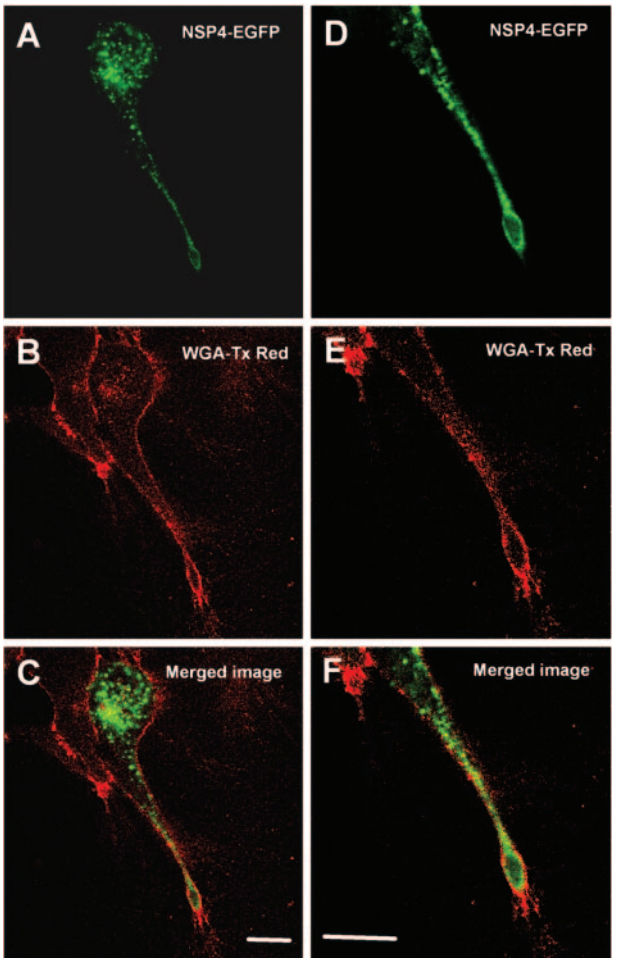

FIG. 8. NSP4-EGFP is localized in the vicinity of, but not in, the plasma membrane of HEK 293 cells. Twenty-four hours postinduction, cells were fixed with 4% formaldehyde, incubated with Texas Red-conjugated wheat germ agglutinin without permeabilization to label glycoproteins in the plasma membrane, and observed by confocal microscopy. (A) NSP4-EGFP fluorescence; (B) plasma membrane staining; (C) merged image of A and B. (D, E, F) cell from images A, B, and C with magnification ×2 to show detail. Bars = 10 μm.

rotavirus-infected cells affects the distribution of other viral proteins, mRNA synthesis, and the formation of viroplasms where viral RNA replicates, suggesting previously unrecognized NSP4 functions in rotavirus replication (18, 26).

These new results raised the questions of where, beyond the ER, iNSP4 is localized and how this non-ER localization of iNSP4 relates to its functions. Studies of iNSP4 localization in rotavirus-infected nonpolarized cells are complicated because cells undergo virus-induced cell lysis 10 to 12 h postinfection. In addition, at early time points (4 h) postinfection, when the extracellular cleaved form of NSP4 is detected (32), intracellular NSP4 is difficult to detect by immunofluorescence beyond the ER. Punctate NSP4 appears with increased expression of all viral proteins and dominates in cells from 6 h postinfection, when the distribution of other viral proteins also changes. This punctate staining was previously interpreted to represent NSP4 in ER membranes that are adjacent to viroplasms, the sites of accumulation of viral proteins where RNA replication occurs (13, 25).

To study iNSP4 localization, we used a simplified model—a HEK 293-derived inducible cell line expressing NSP4 with an EGFP tag fused to its C terminus. A C-terminal fusion was chosen so we would be able to follow localization of the full-length NSP4 as well as the cleavage product of NSP4 (aa 112 to 175) within these cells, since the exact mechanism and location of NSP4 cleavage are not known. Inducible expression was used to produce subcytotoxic concentrations of the fusion protein.

At early time points postinduction, NSP4-EGFP was localized exclusively in the ER and was detected by a rather diffuse distribution pattern colocalizing with the ER markers PDI and calnexin (not shown). The initial ER localization of NSP4-EGFP was consistent with our Western blot analysis of induced HEK 293 cell lysates using anti-NSP4 120–147 antibody where a single major Endo H-sensitive band was detected (Fig. 1). This confirmed efficient ER insertion and glycosylation of the NSP4-EGFP fusion protein. As the NSP4-EGFP expression

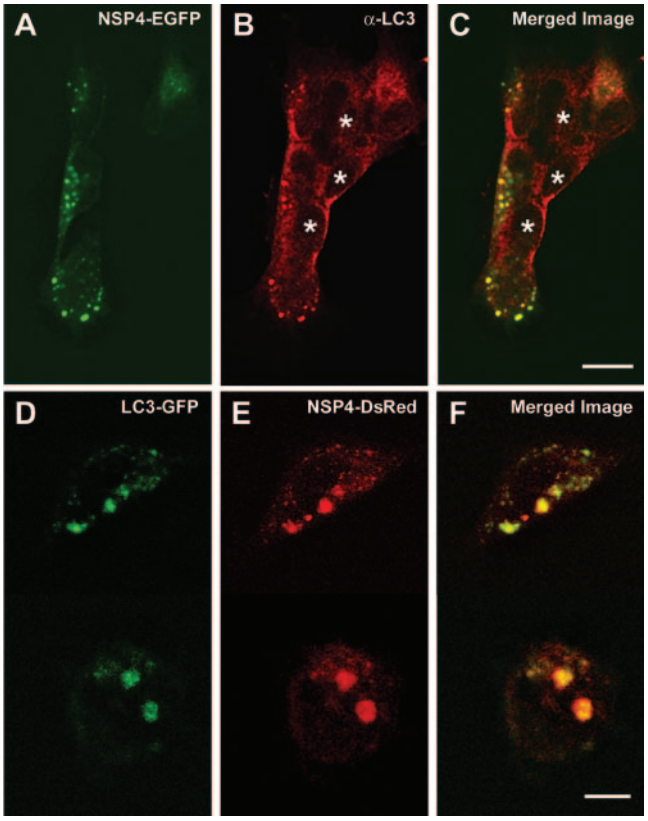

FIG. 9. NSP4-EGFP colocalizes with the autophagosomal marker LC3 in HEK 293 cells. Cells were fixed and permeabilized 24 h postinduction and stained with rabbit anti-LC3 antibody and the Alexa 594-conjugated anti-rabbit secondary antibody. (A) NSP4-EGFP fluorescence; (B) LC3 staining; (C) merged image of A and B. The asterisks mark NSP4-EGFP-negative cells showing a diffuse cytoplasmic staining of LC3. HEK 293 cells were also transiently transfected with a plasmid expressing the LC3-GFP fusion protein and 48 h later with the plasmid expressing NSP4 fused to monomeric red fluorescent protein (Ds2Red). Fixed cells were then observed by confocal microscopy. (D) LC3-GFP fluorescence; (E) NSP4-DsRed fluorescence; (F) merged image of D and E. Panels D, E, and F illustrate two LC3-GFP- and NSP4-DsRed-positive cells acquired separately. Bars = 20 μm and 10 μm, respectively.

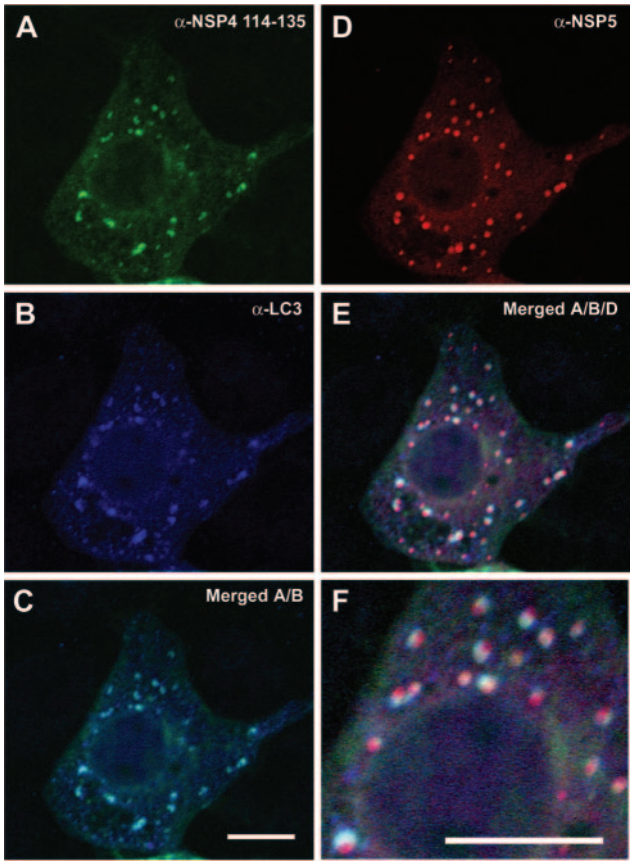

FIG. 10. NSP4- and LC3-positive vesicles associate with viroplasms in rotavirus-infected MA104 cells. MA104 cells were infected with rotavirus strain SA114F at a MOI of 10 and fixed 7 h postinfection. Permeabilized cells were stained with mouse anti-NSP4 114–135 antibody, rabbit anti-LC3 antibody, guinea pig anti-NSP5 antibody, and the corresponding secondary antibodies: Alexa 488-anti-mouse antibody, Alexa 568 anti-guinea pig antibody, and Alexa-647 anti-rabbit antibody. Cells were then observed by confocal microscopy, and acquired images of fluorescence were pseudocolored green, red, and blue, respectively. (A) NSP4 staining; (B) LC3 staining; (C) merged staining of NSP4 and LC3; (D) NSP5 staining; (E) NSP4, NSP5, and LC3 staining; (F) higher (×2.5) magnification of E to illustrate the localization of NSP4 and LC3 relative to NSP5. Bars = 10 μm.

levels increased at the later times postinduction, the fusion protein was detected in vesicles throughout the cytoplasm, in addition to the diffuse ER staining (Fig. 3). PDI and calnexin are two resident ER proteins with different localizations and thus also different staining patterns (ER lumen versus ER membrane). The fact that both of these proteins are excluded from NSP4-EGFP vesicles points to possible exclusion of ER resident proteins from these structures in general.

Only partial colocalization of vesicular NSP4-EGFP with ERGIC-53 and the lack of colocalization with any other known biosynthetic pathway markers suggested that the majority of the NSP4-EGFP vesicles represent a distinct vesicular pool that bifurcates from the ER. This novel vesicular pool does not represent the vesicular tubular clusters found by Xu et al. (31) in Cos-7 cells transiently expressing NSP4, because it failed to label with β-COP and ERGIC 53 and did not align with microtubules but is related to autophagosomes as manifested by colocalization with the autophagosomal marker LC3 (16). Discrepancies between the present study and the study of Xu et al. (31) may be cell type and expression construct specific. To confirm the relevance of our NSP4-EGFP findings with our inducible HEK 293 cell line, we studied the localization of virus-expressed NSP4 in rotavirus-infected cells. In rotavirus-infected MA104 and Cos-7 cells, extensive colocalization of NSP4 with LC3 but only limited colocalization with ERGIC-53 and no colocalization with microtubules during virus replication were observed. An argument can be made that the EGFP tag masks the NSP4 microtubule-binding domain mapped to 54 amino acids at the C terminus of NSP4 (31). However, the fact that our NSP4-EGFP localization does not correlate with the distribution of a microtubule binding mutant of NSP4 (31) argues that simple masking of the microtubule binding site by the EGFP tag is not sufficient to explain localization differences between these studies. Moreover, during virus replication, when other viral proteins are abundant, double-layered

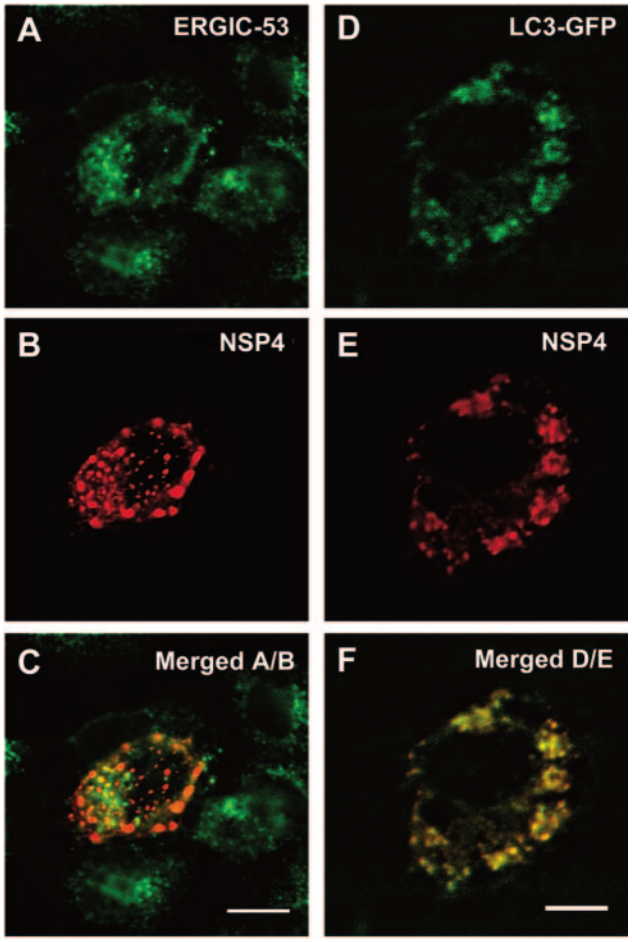

FIG. 11. Limited colocalization of NSP4 with ERGIC-53 and extensive colocalization of NSP4 with LC3 in rotavirus-infected Cos-7 cells. COS-7 cells were infected with rotavirus strain SA114F at a MOI of 10 and fixed 12 h postinfection. Permeabilized cells were stained with rabbit anti-NSP4 120–147 antibody, mouse anti-ERGIC-53 antibody, and the corresponding secondary antibodies: Alexa 488-anti-mouse antibody and Alexa 594 anti-rabbit antibody. Cells were then observed by confocal microscopy. (A) ERGIC-53 staining; (B) NSP4 staining; (C) merged staining of NSP4 and ERGIC-53. (Bar = 10 μm). Cos-7 cells were transiently transfected 48 h prior to infection to express LC3-GFP. Permeabilized cells were stained with rabbit anti-NSP4 120–147 antibody and Alexa 594-conjugated anti-rabbit antibody. (D) LC3-GFP fluorescence; (E) NSP4 staining; (F) merged images of D and E. Bar = 5 μm.

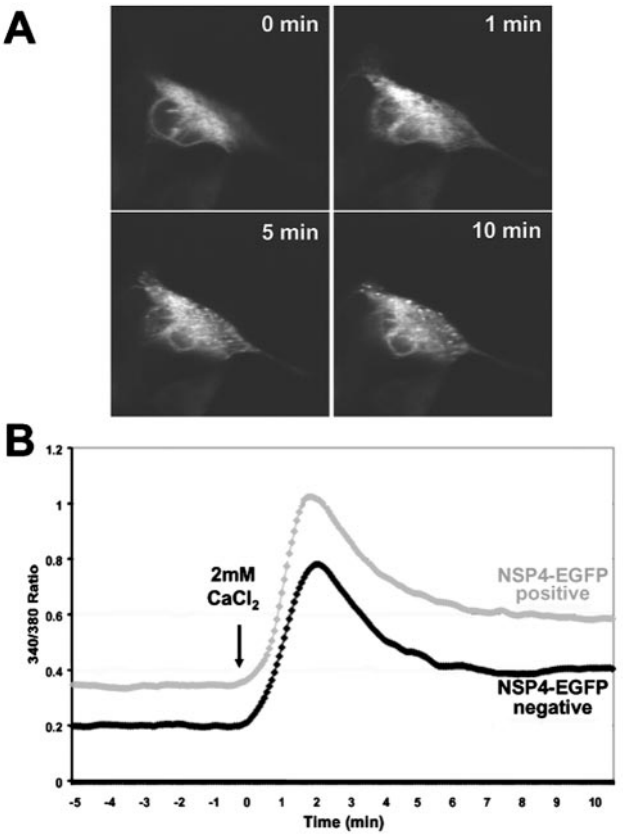

FIG. 12. NSP4-EGFP presence in vesicular structures in HEK 293 cells requires elevated levels of intracellular calcium. Cells were induced and grown for 24 h in calcium-free medium (see Materials and Methods). To normalize extracellular calcium, 2 mM calcium chloride was added to the bath solution at 0 min. (A) Live cells were observed by confocal microscopy, and images were acquired at 0, 1, 5, and 10 min; (B) changes of intracellular calcium upon addition of 2 mM calcium chloride into bathing solution were measured in Fura-2-loaded cells as described in Materials and Methods.

particles and VP4 can bind the C terminus of NSP4 (1, 2), thus blocking access to the microtubule binding site, which may be simulated in our system by the EGFP tag.

We also show here for the first time that formation of the vesicular NSP4-EGFP pool is dependent on increased intracellular concentrations of calcium. Since NSP4-EGFP-induced cells were grown in regular, serum-supplemented medium, formation of the described novel vesicular NSP4 pool is not related to serum starvation, although such vesicles might be up-regulated in rotavirus-infected cells grown in the absence of serum. However, as mentioned above, colocalization of NSP4 and LC3 within vesicles was similar in induced HEK 293 cells and rotavirus-infected MA104 cells grown and maintained in the presence or absence of serum.

The induction and requirement of autophagic vesicles in viral replication has been documented for other RNA viruses, coronaviruses and poliovirus (23, 24, 27). In coronavirus-infected cells, the virus replication machinery associates with LC3-positive ER-derived double-membrane vesicles (23). This association greatly enhances virus replication and is not inhibited by 3-methyladenine, a known inhibitor of autophagy formation (23). In contrast, poliovirus-associated autophagy vesicles are sensitive to 3-methyladenine, and they are positive for LC3 as well as the lysosomal marker LAMP1. Unlike degradative phagolysosomes, polio-induced autophagosome-derived vesicles retain a double membrane and thus are arrested in a prephagolysosomal stage (15). The LC3 marker is also detected in membrane blebs together with the poliovirus capsid protein, implying an additional role of autophagosomes in nonlytic poliovirus release (15). Our results show that rotavirus NSP4 vesicles, which colocalize with the autophagosome-derived vesicle marker LC3, do not colocalize with LAMP1. Further studies are needed to determine if the NSP4 vesicles function in a manner similar to coronavirus-induced autophagy or if these represent a new mechanism by which a viral protein

is capable of inducing or hijacking the cellular autophagy membranes and thus may help in deciphering autophagosomal pathways.

Autophagosomes represent a major organelle recycling pathway in cells (17). Interference with this pathway can have profound effects on cell homeostasis. The NSP4-EGFP-expressing HEK 293 cells possess decreased numbers of lysosomes (Fig. 7D to F). In addition, rotavirus-infected cells have an apparent expansion of reticular membranes (10), which were originally hypothesized to be needed for virus morphogenesis. Our current data suggest that iNSP4 may interfere with autophagosomal maturation (in NSP4-EGFP-expressing and rotavirus-infected cells), which may cause a decrease of the distal organelle pools (lysosomes) and an increase of the size of proximal organelles (ER). Both LC3 and NSP4 bind microtubules (19, 31). LC3 has been proposed to deliver autophagosomes to lysosomes for maturation, and NSP4 has been shown to sequester ERGIC vesicles on microtubules and prevent their fusion with the Golgi apparatus (31). We hypothesize that the association of NSP4 with LC3-positive autophagosomes prevents their fusion with lysosomes, which would otherwise have a detrimental effect on virus replication, and instead, NSP4 recruits autophagosomal membranes to viroplasms to enhance viral replication. Further studies using interfering RNAs or cells lacking key proteins in the autophagy pathway will be needed to test this hypothesis and to determine if rotavirus hijacking of the autophagy pathway has effects similar to or different from those reported for coronavirus and poliovirus.

Based on the data in this paper, we hypothesize that three pools of iNSP4 exist in rotavirus-infected cells, dependent upon the level of NSP4 protein expression. The first pool is represented by NSP4 localized in the ER membrane and is present throughout the course of infection. This pool serves as a receptor for the budding of immature viral particles into the ER, as described previously (1, 20), at the peak of viral infection, when all viral proteins are abundant (after 6 h postinfection). A second, minor pool of NSP4 molecules enters the ERGIC compartment and can be recycled back to the ER or may be a part of the predicted nonclassical secretion pathway for delivery and cleavage of the NSP4 product into the medium of infected cells at early time points postinfection (31), when the levels of viral proteins are relatively low as detected by immunofluorescence (unpublished observation). The third pool of NSP4 molecules, distributed in cytoplasmic vesicular structures associated with the autophagosomal marker LC3 and viroplasms, appears in infected cells at 6 h postinfection, when there is also an increase of intracellular calcium levels due to increased expression of viral proteins (21). We propose that this particular NSP4 pool is involved in regulation of virus replication. Inhibition of NSP4 expression interferes with the formation of large viroplasms and affects viral protein expression (18) and viral mRNA synthesis in rotavirus-infected cells after 6 h postinfection (26). The NSP4 and autophagic marker LC3-positive vesicles, described here, may serve as a lipid membrane scaffold for the formation of large viroplasms by recruiting early viroplasms or viroplasm-like structures formed by NSP2 and NSP5 (12). These NSP4-positive membranes may also function to regulate packaging of the rotavirus genome and transcription through NSP4 association with VP6 on double-layered particles (26).

Our results demonstrate for the first time a calcium-dependent compartmentalization of NSP4 into an autophagosomal pathway arising from a bifurcated ER pool. The ramifications of the involvement of autophagosomal membranes in rotavirus replication or possible release of infectious virus from cells remain to be determined. The fact that NSP4-EGFP localization in our system mirrors localization of NSP4 in virus-infected cells validates the use of our inducible cell line as a new in vitro tool useful for further studies of intracellular NSP4 functions and also as a tool to study regulation of formation and origin of autophagosomal membranes.

ACKNOWLEDGMENTS

This work was supported in part by Public Health Service grants R01 DK30144, DK59550, and DK056338, which supports the Texas Gulf Coast Digestive Disease Center.

We thank members of the Trugnan laboratory for their hospitality and assistance with experiments after Tropical Storm Allison closed laboratories in Houston, Tex., and R. F. Ramig and B. V. V. Prasad for critical comments.

REFERENCES

1. **Au, K. S., W. K. Chan, J. W. Burns, and M. K. Estes.** 1989. Receptor activity of rotavirus nonstructural glycoprotein NS28. J. Virol. **63:**4553–4562.
2. **Au, K. S., N. M. Mattion, and M. K. Estes.** 1993. A subviral particle binding domain on the rotavirus nonstructural glycoprotein NS28. Virology **194:**665–673.
3. **Ball, J. M., P. Tian, C. Q. Zeng, A. P. Morris, and M. K. Estes.** 1996. Age-dependent diarrhea induced by a rotaviral nonstructural glycoprotein. Science **272:**101–104.
4. **Ball, J., D. M. Mitchell, T. F. Gibbons, and R. D. Parr.** 2005. Rotavirus NSP4: a multifunctional viral enterotoxin. Viral Immunol. **18:**27–40.
5. **Berkova, Z., A. P. Morris, and M. K. Estes.** 2003. Cytoplasmic calcium measurement in rotavirus enterotoxin-enhanced green fluorescent protein (NSP4-EGFP) expressing cells loaded with Fura-2. Cell Calcium **34:**55–68.
6. **Both, G. W., J. S. Mattick, and A. R. Bellamy.** 1983. Serotype-specific glycoprotein of simian 11 rotavirus: coding assignment and gene sequence. Proc. Natl. Acad. Sci. USA **80:**3091–3095.
7. **Brostrom, M. A., and C. O. Brostrom.** 2003. Calcium dynamics and endoplasmic reticular function in the regulation of protein synthesis: implications for cell growth and adaptability. Cell Calcium **34:**345–363.
8. **Dong, Y., C. Q. Zeng, J. M. Ball, M. K. Estes, and A. P. Morris.** 1997. The rotavirus enterotoxin NSP4 mobilizes intracellular calcium in human intestinal cells by stimulating phospholipase C-mediated inositol 1,4,5-trisphosphate production. Proc. Natl. Acad. Sci. USA **94:**3960–3965.
9. **Ericson, B. L., D. Y. Graham, B. B. Mason, H. H. Hanssen, and M. K. Estes.** 1983. Two types of glycoprotein precursors are produced by the simian rotavirus SA11. Virology **127:**320–332.
10. **Estes, M. K., E. L. Palmer, and J. F. Objeski.** 1983. Rotaviruses: a review. Curr. Top. Microbiol. Immunol. **105:**124–184.
11. **Estes, M. K., G. Kang, C. Q.-Y. Zeng, S. E. Crawford, and M. Ciarlet.** 2001. Pathogenesis of rotavirus gastroenteritis. *In* D. Chadwick and J. Goode (ed.), Gastroenteritis viruses. Novartis Found. Symp. **238:**82–100.
12. **Fabbretti, E., I. Afrikanova, F. Vascotto, and O. R. Burrone.** 1999. Two non-structural rotavirus proteins, NSP2 and NSP5, form viroplasm-like structures in vivo. J. Gen. Virol. **80:**333–339.
13. **Gonzàles, R. A., R. Espinosa, P. Romero, S. López, and C. F. Arias.** 2000. Relative localization of viroplasmic end endoplasmic reticulum-resident rotavirus proteins in infected cells. Arch. Virol. **145:**1963–1973.
14. **Haughland, R. P.** 1996. Handbook of fluorescent probes and research chemicals, 6th ed. Molecular Probes, Eugene, Ore.
15. **Jackson, W. T., T. H. Giddings, Jr., M. P. Taylor, S. Mulinayawe, M. Rabinovitch, R. R. Kopito, and K. Kirkegaard.** 2005. Subversion of cellular autophagosomal machinery by RNA viruses. PLOS Biol. **3:**861–871.
16. **Kabeya, Y., N. Mizushima, T. Ueno, A. Yamamoto, T. Kirisako, T. Noda, E. Kominami, Y. Ohsumi, and T. Yoshimori.** 2000. LC3, a mammalian homologue of yeast Apg8p, is localized in autophagosome membranes after processing. EMBO J. **19:**5720–5728.
17. **Klionsky, D. J., and S. D. Emr.** 2000. Autophagy as a regulated pathway of cellular degradation. Science **290:**1717–1721.
18. **López, T., M. Camacho, M. Zayas, R. Nájera, R. Sánchez, C. F. Arias, and S. López.** 2005. Silencing the morphogenesis of rotavirus. J. Virol. **79:**184–192.

19. **Mann, S. S., and J. A. Hammarback.** 1994. Molecular characterization of light chain 3. A microtubule binding subunit of MAP1A and MAP1B. J. Biol. Chem. **269:**11492–11497.
20. **Meyer, J. C., C. C. Bergmann, and A. R. Bellamy.** 1989. Interaction of rotavirus cores with the nonstructural glycoprotein NS28. Virology **171:**98–107.
21. **Michelangeli, F., M. C. Ruiz, J. R. del Castillo, J. E. Ludert, and F. Liprandi.** 1991. Effect of rotavirus infection on intracellular calcium homeostasis in cultured cells. Virology **181:**520–527.
22. **Morris, A. P., J. K. Scott, J. M. Ball, C. Q. Zeng, W. K. O'Neal, and M. K. Estes.** 1999. NSP4 elicits age-dependent diarrhea and $Ca^{(2+)}$mediated I(−) influx into intestinal crypts of CF mice. Am. J. Physiol. **277:**G431–G444.
23. **Prentice, E., W. G. Jerome, T. Yoshimori, N. Mizushima, and M. R. Denison.** 2004. Coronavirus replication complex formation utilizes components of cellular macrophagy. J. Cell Biol. **279:**10136–10141.
24. **Schlegel, A., T. H. Giddings, Jr., M. S. Ladinsky, and K. Kirkegaard.** 1996. Cellular origin and ultrastructure of membranes induced during poliovirus infection. J. Virol. **70:**6576–6588.
25. **Silvestri, L. S., Z. R. Taraporewala, and J. T. Patton.** 2004. Rotavirus replication: plus-sense templates for double-stranded RNA synthesis are made in viroplasms. J. Virol. **78:**7763–7774.
26. **Silvestri, L. S., M. A. Tortorici, R. Vasquez-DelCaprio, and J. T. Patton.** 2005. The rotavirus glycoprotein NSP4 is a modulator of viral transcription in the infected cell. J. Virol., in press.
27. **Suhy, D. A., T. H. Giddings, Jr., and K. Kirkegaard.** 2000. Remodeling the endoplasmic reticulum by poliovirus infection and by individual viral proteins: an autophagy-like origin for virus-induced vesicles. J. Virol. **74:**8953–8965.
28. **Tian, P., A. Ottaiano, P. A. Reilly, S. Udem, and T. Zamb.** 2000. The authentic sequence of rotavirus SA11 nonstructural protein NSP4. Virus Res. **66:**117–122.
29. **Welch, W. S. K., S. E. Crawford, and M. K. Estes.** 1989. Rotavirus SA11 genome segment 11 protein is a nonstructural phosphoprotein. J. Virol. **63:**3974–3982.
30. **Xu, A., A. R. Bellamy, and J. A. Taylor.** 1998. BiP (GRP78) and endoplasmin (GRP94) are induced following rotavirus infection and bind transiently to an endoplasmic reticulum-localized virion component. J. Virol. **72:**9865–9872.
31. **Xu, A., A. R. Bellamy, and J. A. Taylor.** 2000. Immobilization of the early secretory pathway by a virus glycoprotein that binds to microtubules. EMBO J. **19:**6465–6474.
32. **Zhang, M., C. Q. Zeng, A. P. Morris, and M. K. Estes.** 2000. A functional NSP4 enterotoxin peptide secreted from rotavirus-infected cells. J. Virol. **74:**11663–11670.